



Pixel Detector Mechanics Conceptual Design Review

ATLAS Project Document No:

ATL-IP-ES-0018

Institute Document No.

Created: **24/06/2001**

Page: **1 of 2**

Modified:

Rev. No.: **1**

Technical Specification

Pixel Detector Global Support Frame

Abstract

This document describes the technical specifications for the design and fabrication of the global support frame for the ATLAS pixel detector.

Prepared by:

E. Anderssen, M. Gilchriese, W. Miller

Checked by:

Approved by:

Distribution List

History of Changes

<i>Rev. No.</i>	<i>Date</i>	<i>Pages</i>	<i>Description of changes</i>

Table of Contents

1	INTRODUCTION.....	4
2	DIMENSIONS AND ENVELOPES.....	4
2.1	Disk Support Rings.....	6
2.2	Layer 1 and Layer 2 Barrel Shells	6
2.3	B-layer Support Shell.....	6
2.4	Mounts To SCT	6
2.5	Services.....	7
2.6	Services Support Panels	7
2.7	Pixel Support Tube.....	7
3	FINAL ASSEMBLY.....	7
4	SURVEY REQUIREMENTS.....	7
5	LOAD CONDITIONS, STABILITY AND ANALYSIS	8
6	OTHER REQUIREMENTS.....	9
7	MATERIALS	9
8	QUALIFICATION TESTS	10
8.1	Material Coupon Testing.....	10
8.2	As-built Dimensions.....	10
8.3	Load Tests.....	10
8.4	Assembly Test.....	10
9	QUALITY ASSURANCE.....	10

1 Introduction

The global support frame consists of a flat-panel space frame in three sections - a barrel section and two, identical disk sections as shown in Figure 1. These sections are joined to make the complete frame.



Figure 1. ATLAS Pixel global support frame, which consists of three sections - barrel and two disk sections. The barrel and two disk sections are shown joined on the left. One of the support cones for the barrel shells is shown in the right model.

Included in the barrel section are two End Cone supports for the barrel shells as also shown in Figure 1.

A complete prototype disk section of the global support frame has been fabricated and tested. A prototype of an End Cone is under fabrication and test.

The three sections of the support frame and the two End Cones will be fabricated by a vendor under contract to LBNL.

2 Dimensions and Envelopes

The current baseline dimensions of the global support frame are shown in Figure 2. Detailed envelopes will be addressed later in the creation of fabrication drawings for the global support sections. The current envelopes for the radial dimensions of the global support exceed the nominal by 0.5 mm both on the inner and outer surfaces. The envelope for the total length is also 0.5mm(each side) greater than the nominal dimensions

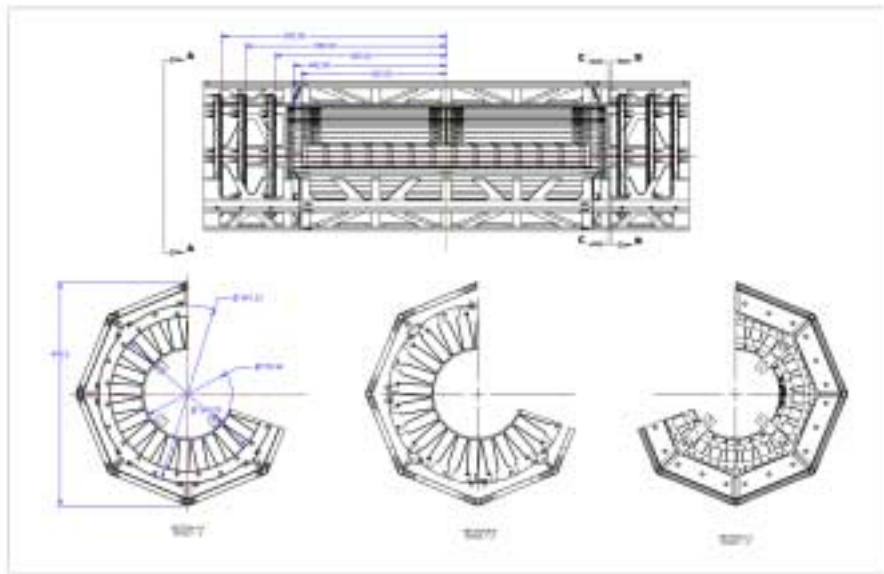


Figure 2. Current baseline dimensions of the barrel and disk sections of the global support frame.

The current baseline dimensions of the End Cones are shown in Figure 3 and Figure 4.

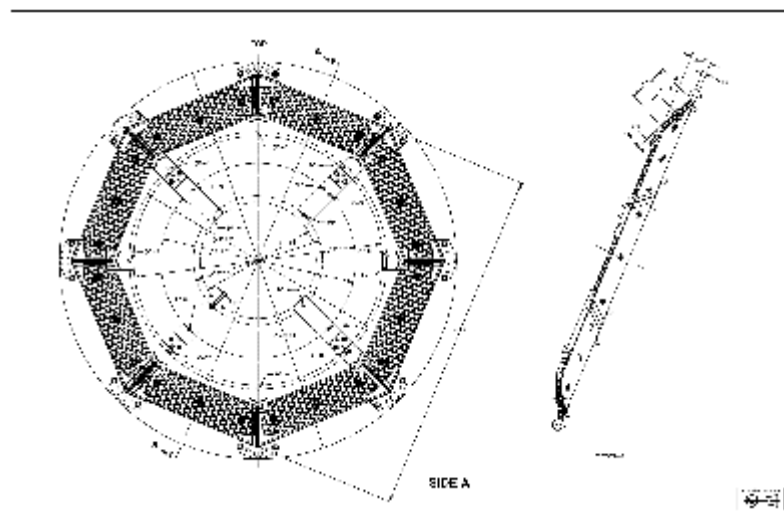


Figure 3. Current baseline dimensions of the End Cone, side A.

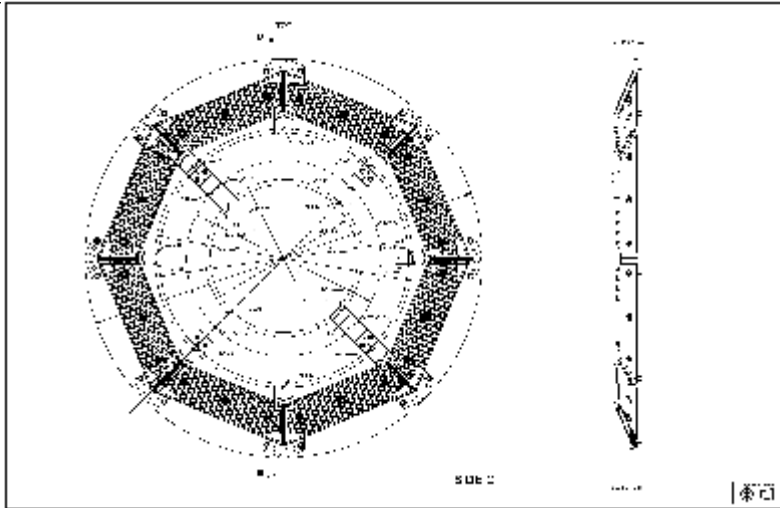


Figure 4: Current dimensions of the End Cone, Side C.

3 Interfaces

The principal interfaces to the global support frame are (1) the disk support rings; (2) the Layer 1 and Layer 2 barrel, stave support shells; (3) the B-layer support shell; (4) the mounting structure to attach the global support frame to the SCT barrel structure; (5) services(cables and pipes) from the modules mounted on the barrel staves and disk sectors; (6) services support panels that hold services within the pixel support tube; and (7) to the pixel support tube(PST).

3.1 Disk Support Rings

Interfaces to the disk support rings are covered in the Technical Specification for the Disk Support Rings.¹

3.2 Layer 1 and Layer 2 Barrel Shells

Interfaces to these shells are covered in the Technical Specification for the Layer 1 and Layer 2 Barrel Shells.²

3.3 B-layer Support Shell.

Eric can you provide something eg. a figure for this and some short text. If we don't know just say not defined at this time.

Figure 5. B-layer shell interface region.

3.4 Mounts To SCT

The global support frame is attached to the SCT barrel structure at four locations. The mounting conditions are shown in Figure 6(**Eric please provide**).

Figure 6. Support conditions for the global support frame attached to the SCT barrel structure.

A preliminary definition of the dimensional interfaces to the SCT structure are shown in Figure 7(**Eric please provide figure and short text if needed**).

Figure 7. Dimensional interfaces of the global support frame to the SCT barrel structure.

3.5 Services

Barrel electrical services and coolant piping run from the ends of the bi-stave assemblies across the support cone, through a gap between the barrel and disk sections of the frame, and then along the outside of the disk sections of the frame. Disk electrical services run along the inside of the disk sections of the frame. Strain relief fixtures will be attached to the endcones and to the disk sections using a regular array of PEEK inserts for support of the fixtures. The location of these inserts is fixed for the End Cone(see Figure 3 and Figure 4) but remains to be determined for the disk frame sections.

3.6 Services Support Panels

Services support panels hold cables and pipes inside the PST and slide with the global support frame inside the PST during installation or removal. There is a mechanical connection between each end of the global support frame and the service panels so that they may slide together inside the PST. The design of this interface does not yet exist. The fabrication of these interfaces pieces is the responsibility of LBNL, not the vendor manufacturing the global support frame.

3.7 Pixel Support Tube

The global support frame slides on four riders attached at the ends of the frame on the detector V- and flat-rails inside the PST. The design of this interface does not yet exist. The fabrication of these riders is the responsibility of LBNL, not the vendor manufacturing the global support frame.

4 Final Assembly

The End Cones and barrel shells are mounted in to the barrel section of the support frame. No design exists yet for the tooling and procedures needed for this assembly step. The disks are mounted into the disk section and the disk sections are joined to the barrel section as illustrated in Figure 8.



Figure 8. Illustration of the method for joining the barrel and disk sections of the support frame.

An initial conceptual design for the procedures necessary to mount the disks and to join the disk and barrel sections has been done and is illustrated at <http://www-atlas.lbl.gov/~goozen/assdetset.html>. Attachment of tooling for barrel and disk assembly, and for joining the barrel and disk sections, will be made to the corner blocks in the frame sections shown in Figure 8.

5 Survey Requirements

The locations of the pixel modules must be referenced to the mounting structure connecting the global support frame to the SCT barrel structure. This is to be done in multiple steps

- Modules referenced to the local supports(staves and disk sectors)
- Local supports referenced to the intermediate supports(barrel shells and disk rings)
- Intermediate supports referenced to the global support frame - to survey references mounted in or attached to the corner blocks in each section

- Support frame referenced to SCT mounts after final assembly of the barrel and disk sections.

The procedures, survey markers and tools for accomplishing the surveys referenced to the support frame have not yet been developed.

6 Load Conditions, Stability and Analysis

The conceptual analysis of the Global Support frame has been completed. The objective of the analysis was to confirm that reducing the frame dimensions from the original baseline did not invalidate the extensive analysis and prototype testing conducted previously. This task was accomplished.

Stability requirements are estimated assuming a maximum of 20% degradation in the (rms) ϕ , R or Z measurements. The "stability budget" is arbitrarily apportioned among the local supports(staves or sectors), intermediate supports(shells or rings) and the support frame. Tolerances are assumed to be $\sqrt{12}$ x the rms value. In the barrel region, the apportionment is 8:1:1 for stave, shell and frame, respectively. In the disk region, it is 1:2:4 for sector, ring and frame, respectively. The tolerance(rms) values are given in Table 1.

The recent analysis³ of the Global Supports conceptual design specifically addressed gravitational loading, dynamic stiffness, and torsional stiffness. Gravitational sag is of concern in the context of maintaining detector alignment. Dynamic stiffness on the other hand quantifies the susceptibility of the detector to unforeseen vibration. Torsional stiffness is assessed to ascertain what level of disturbance is required to twist the detector assembly. The final Global Support configuration incorporated end plate stiffening panels to provide radial stiffness in the plane of Pixel to SCT support. The total mass of the structure and non-structure mass derived from the FE model was 28.89kg, with the two end plate stiffeners being 0.25kg.

Stability Item	Tolerance(rms) in microns	Analysis
Radial and lateral motion -"R"	Disk: 200(58) Barrel: 5(1.5)	Gravitational sag-11.5 μ m; response to random vibration in R \ll 1 μ m (lateral motion suppressed by frame end plate)
Tangential motion-" ϕ "	Disk: 24(7) Barrel: 1.8(0.5)	ϕ -position set by planarity and rigidity the frame 4-point supports, detector twist with 1-support point removed is limited to 53.5 μ m
Axial motion-"Z"	Disk: 425(122) Barrel: 14(4)	Thermal length change \sim 1.4 μ m/ $^{\circ}$ C

Table 1. Stability tolerance(rms) values for barrel and disk regions and estimates of frame motions.

Internally, relative positional change between the pixel disks and the barrel detector elements is controlled by using materials with very low coefficients of thermal expansion (CTE), in most cases approaching zero CTE. Temperature control of the evaporative coolant system, ensures virtually no change in length or radial position between the pixel sections, the disk array and staves. Initially, the detector will potentially expand in length 56 μ m when cooling from room temperature to -15 $^{\circ}$ C, thereafter the sensitivity in Z to a change temperature is less than 1.4 μ m/ $^{\circ}$ C. Consequently, from outer disk array to outer disk array for a 5 $^{\circ}$ C change (cyclical in time, short term periodicity) the detector stability is within 7 μ m, well within the stability limit of 425 μ m for Z. Radial positional changes due to the same effect is much less. Time varying, spatial temperature changes that cause bending of the frame have not been address. This effect is anticipated to be within the required limits because the global CTE effect is small. This effect will be evaluated once the Pixel Detector system is completely defined.

The detector vibration stability without reinforcing end plates is marginal. If exposed to a harmonic input of 0.01G's the detector motion would be less than 10 μ m laterally, and 2.82 μ m if subjected to a random vibration. The response may grow to an unacceptable amount if the fundamental mode dropped to roughly 30Hz. The non-structural mass from services, strain relief, etc., is expected to increase above the current assumed values, during the preliminary design phase. An increase in non-structural mass impacts frame dynamic stiffness, lowering the frame fundamental mode. To offset this prospect, end reinforcement plates were added to raise the fundamental mode to 89Hz, above potential vibration sources. These plates, at this stage of our design formulation, ensure vibration will not be a stability issue, unless non-structural mass grows out of expected proportions. Of equal importance, these plates simplify the design of the connection between the Global Support frame and the Pixel Detector Support tube.

7 Other Requirements

The sections of the global support frame will be coated with Parylene(0.008-0.012 mm thick) after fabrication to contain conducting carbon dust or fragments.

8 Materials

The materials of construction to be used in constructing the Global Support frame and sub-components will use commercially available composite materials. The outer frame, end cones, and end plate reinforcement panels use a sandwich construction. All sandwich facings will use very high modulus pitch based graphite fibers for maximum stiffness. Prototype frame tests were conducted with a quasi-isotropic panel composed of XN80 (Nippon) fibers and EX1515 cyanate ester resin from Bryte Technology. (It appears that Nippon is replacing the XN fiber series with their new fiber series, designated YSH). Recent prototypes have been constructed with the YSH 50, a replacement for XN50 and M55J. Results of the prototype tests were satisfactory and met our expectations. Table 2 lists the materials chosen for the Global Support frame.

Table 2. Global Support Frame Materials

Global Support Frame Item	Material
Outer Frame	
Sandwich Facings	YSH90 unitape with RS3 or EX1515 cyanate ester resin, quasi-isotropic laminate
Honeycomb Core	XN50 woven cloth/cyanate ester resin, by YLA Cellular, 6.35mm cell, density 48kg/m ³
Vertex Corner Mounts (frame section connections)	YSH50 woven cloth and RS3 cyanate ester resin laminate
Corner Tubes	YSH90 unitape and RS3 cyanate ester resin
Corner Splice	YSH90 unitape and RS3 cyanate ester resin
Vertex Joint Inserts	Aluminum
End Cones	
Sandwich Facings	YSH90 or P30cyanate ester quasi-isotropic laminate
Honeycomb Core	XN50/cyanate ester resin, by YLA Cellular, 6.35mm cell, 48kg/m ³
Inner and Outer Mounting Tabs	YSH50/RS3 cyanate ester
End Plates	Same materials as end cone

9 Qualification Tests

Qualifications tests are to be performed by the fabrication vendor on materials to be used in the ring construction and on each ring after fabrication. LBNL will also perform qualification tests.

9.1 Material Coupon Testing

Tensile test coupons will be cut from a sample of the laminates (0.43mm thick) prepared for the sandwich facings. Tensile tests, for tensile modulus and strength, will be performed to ASTM D3039. No specialized tests are planned for solid laminate material (4mm thick) used in the support tabs and mounting connections.

9.2 As-built Dimensions

The fabrication vendor will measure the as-built dimensions of the subcomponents (flat panels, etc) before assembly of the individual frame sections. The as-built dimensions will also be measured by the vendor and cross checked by LBNL.

9.3 Load Tests

A static load will be performed on each completed outer frame section. The test will be a simple cantilever test, to 1.5 times the required load transfer between frame sections. The test will verify the structural integrity of the composite construction.

A separate static load test of the complete outer Global Support frame will be performed. Non-structural mass equivalent to 1.5 times design load will be added to the frame, at the appropriate Z locations. The static load test will verify the structural design and validate the fabrication quality.

9.4 Assembly Test

A trial assembly of the endcones to the barrel section and of the disk sections to the barrel section (with endcone) will be done by the fabrication vendor and by LBNL. It is planned to have a trial assembly of the intermediate supports into the support frame as well.

10 Quality Assurance

The fabrication vendor will provide a quality control plan to LBNL as part of the fabrication contract.

¹ ATL-IP-ES-0025, "Technical Specification for Pixel Detector Disk Support Rings". June 2001.

² ATL-IP-CS-0007, "Specification for Barrel Layer 1 and 2 Support Structures", November 2000.

³ W. O. Miller, Structural Analysis of ATLAS Pixel Detector Global Support Frame-432mm Envelope, HTN-106210-0002, HYTEC, Inc., dated May 18, 2001



Structural Analysis of ATLAS Pixel Detector Global Support Frame-432mm Envelope

W. O. Miller

5/18/2001

Abstract

The ATLAS-LHC Pixel Detector Global Support Structure has been re-designed to provide a provision for remote insertion of the fully assembled detector. The Global Support structure is composed of an outer frame, two end cones for supporting the inner barrel shells, 6-circular rings for supporting the pixel sectors, and the associated mounts for the support rings. The size of this system is now considerably smaller, but the length remains unchanged. The non-structural mass supported by the frame structure is expected to decrease with the new size requirement, but not necessarily linearly with geometrical changes. Thus, a complete new evaluation of the frame structural aspects was undertaken. The inner barrel shells are not part of this study. Finite element model results that characterize strictly structural aspects of the Global Support Structure Outer Frame and End Cones are reported. Interface details between the basic structure and the detector support outer shell are not complete at this time. In addition, interface information is needed on the B-Layer, the innermost pixel layer in the barrel region. Further analytical studies are warranted to complete this structural assessment when this information becomes available.

DESIGN ENGINEERING
ADVANCED COMPOSITE APPLICATIONS
ULTRA-STABLE PLATFORMS

110 EASTGATE DR.
LOS ALAMOS, NM 87544

PHONE 505 661-3000
FAX 505 662-5179
WWW.HYTECING.COM

Table of Contents

1. Introduction	3
2. Discussion	3
2.1 End Cone	3
2.2 Outer Frame	5
2.3 Frame Dynamic Solutions	6
2.4 Global Support Assembly Dynamic Solutions	8
2.5 Global Support Assembly Static Solution	12
2.6 Global Support Frame with an End Reinforcement Plate	13
3. Recommendations	15

1. Introduction

A finite element model was constructed directly from the Solid-Works (SW) 3D CAD file of the frame geometry under consideration for ATLAS. This step ensured that the detail representing the cutout pattern in the outer frame structure and end cone geometry was correct; in addition, this step simplified the model generation. COSMOS/Works, a seamless interface of COSMOSM and SW, was used to create mid plane surfaces for the outer frame and end cone structural elements. COSMOS/M was used to mesh the surface geometry, and for obtaining the static and dynamic solutions. A beam element (3D) representation of the disk support rings and disk support ring mounts was added to the shell model.

2. Discussion

2.1 End Cone

Before proceeding with the complete frame ensemble, a finite model of the end cone was created and analyzed with COSMOS/M. This model is shown in Figure 1. Both static and dynamic (eigenvalue extraction) analyses were made.

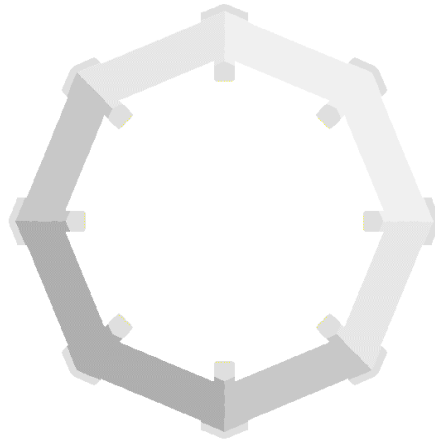


Figure 1: End Cone FE model prepared using COSMOS/M. Geometry definition was derived from a Solid Works 3D model of the ATLAS Pixel Detector. Model is composed of 15,492 elements, a combination of Shell4L and Shell4. Total number of nodes is 6659

An assessment was made of the static deflection of end cone under the weight of 8kg normal to the end cone inner mounting tabs. These tabs are used for supporting the inner barrel structures. A static deflection of $1.55\mu\text{m}$ was obtained from this loading condition. The end cone mass is a small fraction of this total (0.15kg), thus this load alone defines the stiffness. The fundamental frequency normal (Z) to the end cone is set by this value of mass and the end cone

stiffness. Since the stiffness is equal to $k = \frac{F}{\Delta Z}$ and a 1DOF frequency estimate is given by

$f = \frac{1}{2\pi} \sqrt{\frac{k}{M}}$, we see that $f = \frac{1}{2\pi} \sqrt{\frac{1}{\Delta Z}}$. Thus, our estimate of the first mode is 127.8Hz.

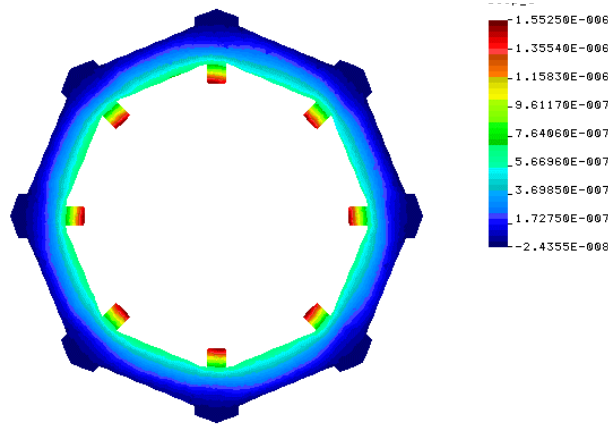


Figure 2: Deformation (peak 1.55 μ m) from gravity load along Z-axis for the End Cone FE model with a concentrated mass of 8kg distributed at the 8-inner mounting tabs. Mounting tabs simulate location of the outermost pixel barrel layer. All outer supports fixed in XYZ.

Results of the end cone modal analysis are presented in Figure 3, Figure 4, and Figure 5. First, the fundamental mode for the cone alone is shown, 2283.8Hz. Next, the effect of adding the mass anticipated for two barrel Layers 1 and 2 is shown; the frequency drops dramatically to 136.7Hz. In the last figure, we illustrate this effect on axial frequency, and show the simple 1DOF model described above superimposed, although offset for clarity. We note that for an 8kg mass that the frequency is nominally 129Hz, which is quite close to our 1DOF model estimate above.

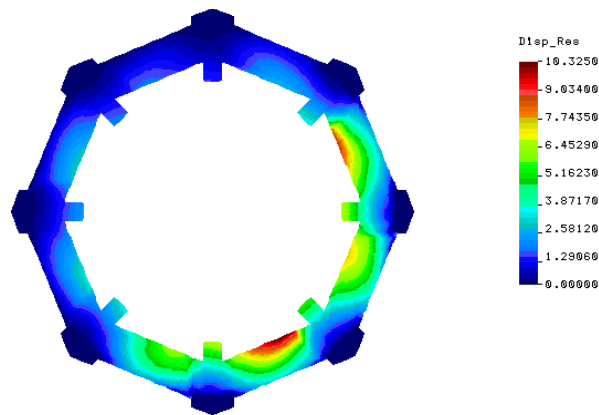


Figure 3: Fundamental vibration mode of 2283.8Hz for the End Cone FE model based on all composite material. Model end cone mass of 0.15kg; the outer supports are fixed in XYZ.

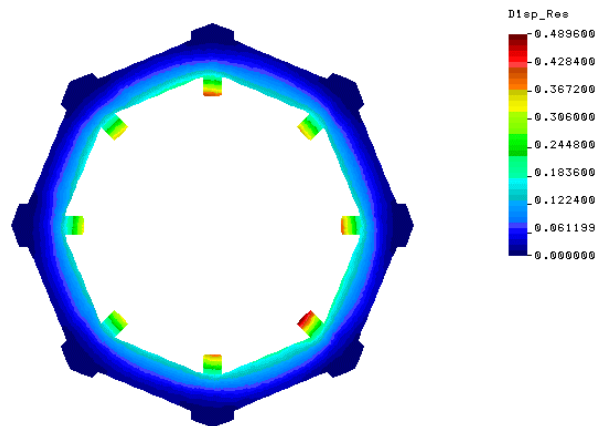


Figure 4: Fundamental vibration mode of 136.7Hz for the End Cone FE model based on all composite material. Model mass of 7.30kg; the outer supports are fixed in XYZ. Mass of 7.15kg per end cone is distributed at the 8-inner shell support fingers. Mass addition is to simulate the pixel detector barrel components.

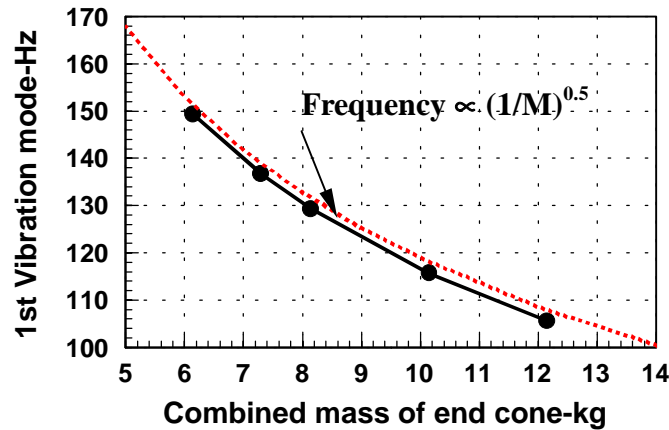


Figure 5: Series of FE end cone model solutions illustrating the effect of added mass on the 1st vibration mode. Outer eight corners of end cone are fixed in XYZ. Curve in red depicts the dependency of a single degree of freedom spring-mass model where for a fixed stiffness the frequency changes inversely proportional to the square of mass.

2.2 Outer Frame

The finite element model of the outer frame is shown in Figure 6. This model is composed of quadrilateral shell elements, Shell4L for the sandwich laminates and Shell4 for the solid laminates, and 3D beam elements for the longitudinal tubes in the frame corners. The structural mass for this frame geometry is 2.85kg, roughly a 1kg less than the larger (500mm dia.) frame studied previously.

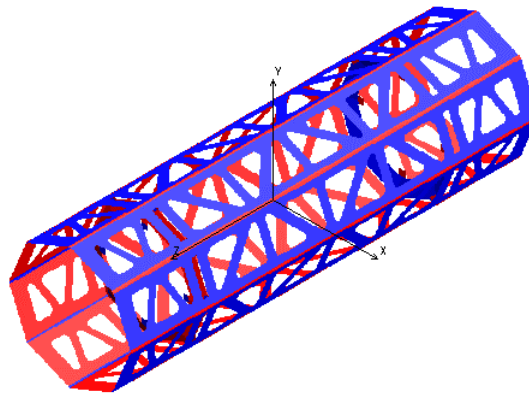


Figure 6: Outer frame and end cone FE model. Model consists of 33,546 Shell4L, Shell4, and 3D Beam elements. Total number of nodes is 29,806. The mass of the frame representation is 2.85kg.

2.3 Frame Dynamic Solutions

Figure 7 depicts the modal shape for the fundamental frame mode, lateral sway. The boundary constraints on the frame corners for this solution are XYZ, XY, YZ, and Y. The XYZ and XY constraints are on the same side; these are evident by the blue shade, denoting zero motion. Since the frame on the left side is free to move in the X-direction, the lateral motion becomes a dominant mode. These boundary conditions were chosen to be consistent with the previous frame FEA studies. At some point, the BC's must be reconciled with the design of the support mounts at the 4-corners.

The frequency of the first mode can be raised by simply moving the support points to a plane even with the two end cones. However, at this early juncture in the design of the support system we do not know how practical this might be or what implications this decision may have on the overall mounting of the Pixel Detector in the SCT.

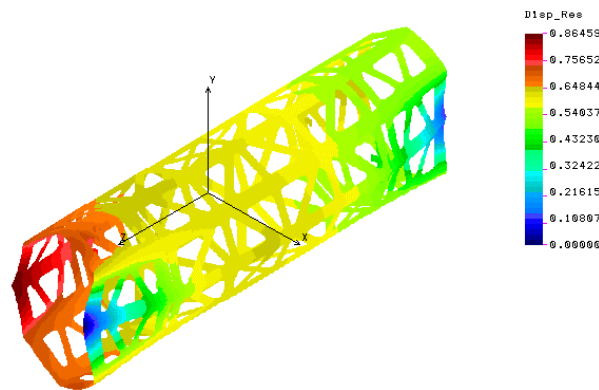


Figure 7: First mode of the Outer Frame/End Cone FE model. Fundamental mode is a sway mode of 149.71Hz, against the corner restraints. Restraints at the 4-corners, front to back, is XYZ, XY, YZ, Y. The Y restraint is at the upper, back corner. Mass of structural components is 2.85kg.

Figure 8 reflects the addition of the disk support rings and ring mounts to the overall frame model. The mass has increased slightly, but the general characteristic remains the same.

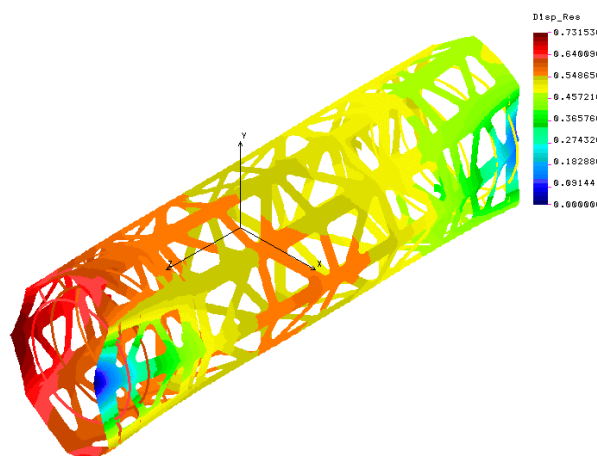


Figure 8: First mode of the Outer Frame/End Cone FE model with the 6-Disk Support Rings added. Fundamental mode is a sway mode of 147.67Hz, against the

corner restraints. Restraints at the 4-corners, front to back, is XYZ, XY, YZ, Y. The Y restraint is at the upper, back corner. Combined mass of the system is 3.6kg.

At this point, we chose to examine the axial stiffness of the disk support ring as modeled in the frame. The disk support ring is connected to the frame with 3D beam elements with section properties that are intended to model the PEEK adjustable mounts. Figure 9 illustrates a comparison between the results on a detailed shell model of the ring alone and the frame model. A 1N force was applied in both cases to the ring midway between supports. In the shell model, case on the left, the ring is fixed at the location of the spherical ball on the ring. In frame model on the right, the ring is subject to the compliance of ring mounts, as well as the frame. Compliance in the frame stems from the connection of the PEEK mounts to the longitudinal tubes in the outer frame structure. We see a small acceptable increase in compliance.

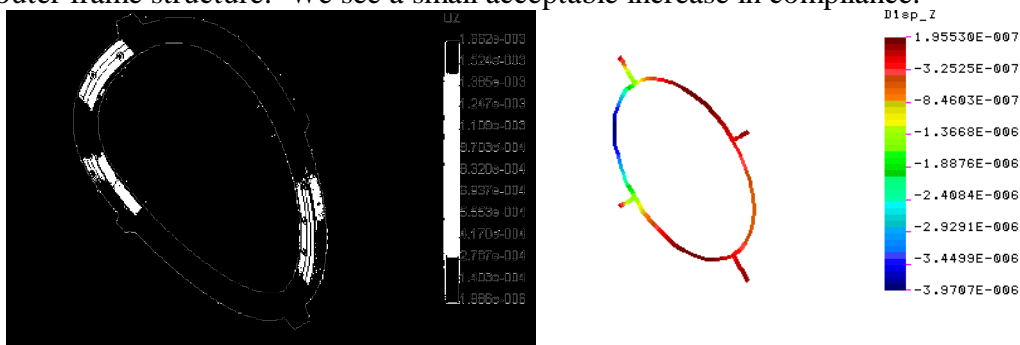


Figure 9: Comparison between two separate Disk Support Ring FE models, the left being a highly refined shell element model and the right a 3D beam model used as part of the Global Support Frame FE model. The result on the right also incorporates 3D beam elements, which simulate the PEEK mount connections to the frame. The shell model lacks the complete mount definition. For 1N force exerted at mid span between mounts the deflections are 1.66 μ m (on left) and 3.97 μ m (on right) respectively. (Force was exerted in opposite directions in the two models)

2.4 Global Support Assembly Dynamic Solutions

Figure 10 depicts the solution for frame system with the sector mass added. The total mass is now 5.76kg and the frequency has dropped to 113.83Hz. The earlier solution showed that the disk support rings do not contribute radial stiffness to the frame, a contribution needed to suppress the first mode or to raise the frequency noticeably.

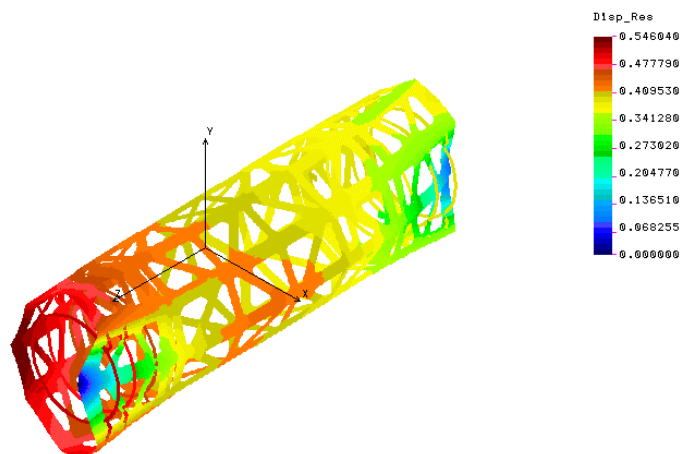


Figure 10: Fundamental mode for Global Support Frame with Disk Support Rings and Pixel Sector mass (45g) included. Total mass of system is 5.76kg and the resultant frequency is 113.83Hz, in a lateral sway mode. The rings do not contribute stiffness to the frame, as evidenced by their lack of distortion.

A compelling reason for seeking increased radial stiffness is shown when the mass of the first two layers of the barrel region are added, Figure 11. Now the frequency has dropped to 61.59Hz. We must now be concerned about the actual dynamic response. Our objective is to limit the motion of the Pixel Detector relative to the SCT detector axis to less than 10 μ m.

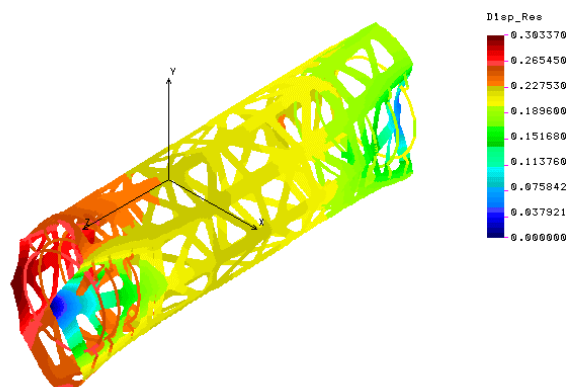


Figure 11: Fundamental mode for Global Support Frame with Disk Support Rings and Pixel Sector mass (45g) included and Pixel Barrel-2 layers plus staves and stave services¹. Total mass of system is 20.03kg; resultant frequency is 61.59Hz, in a lateral sway mode. As before, the rings do not contribute stiffness to the frame, as evidenced by their lack of their distortion.

One will note that the frequency drop between Figure 10 and Figure 11 is proportional to:

¹ Estimate for the barrel components was derived from the old Global Support FEA. Thus, the total mass for the system in this solution is too low.

$$\frac{f_{new}}{f_{old}} \approx \sqrt{\frac{M_{old}}{M_{new}}}$$
; indication that a further decrease can be anticipated when corrections are

made to the overall mass, which is needed to account for increased non-structural mass associated with the stave services and the B-layer mass. The massive barrel region is being treated as a non-structural mass, which produces this effect. If the addition of the barrel services and the B-layer were to increase the system mass to say 34kg, the frequency of the first mode can be expected to drop significantly.

The most recent estimate for the system mass, including frame structure, used in the FE model is 24.64kg. Figure 12 depicts the mode shape and frequency for this configuration. The frequency is now below 60Hz (55.48Hz). It is appropriate now to investigate what this low frequency means in terms of dynamic response.

First, one must realize that it is difficult, and somewhat subjective, to quantify what vibration level we can expect. There have been no vibration surveys made for ATLAS, to our knowledge. However, we anticipate that there will be both a random component and discrete harmonic spikes. Our previous review of a CERN report on the L3 Experiment indicated that both were present.

The Pixel Detector is the innermost component of a very large complex detector so the extent to which the background random vibration is either amplified or attenuated is difficult to surmise. Thus, to conservatively (hopefully) estimate the response we collected data on various experimental halls that were designed with isolation in mind, and to this spectra we add a conservative factor. The result of our attempt to quantify an appropriate random input spectrum is shown in Figure 13.

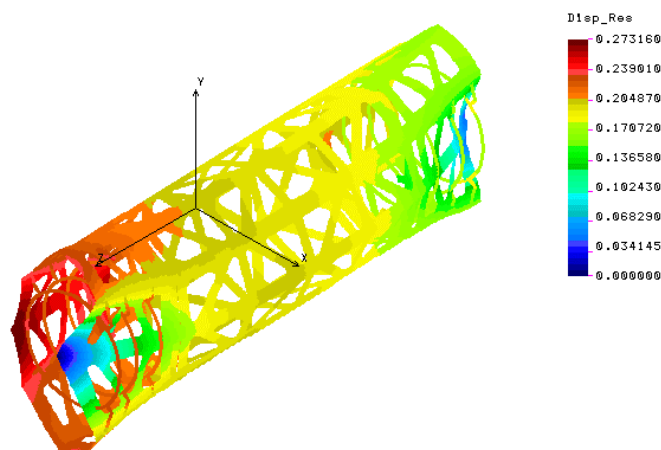


Figure 12: Fundamental mode for Global Support Frame with Disk Support Rings and Pixel Sector mass (45g) included and Pixel Barrel layers (inc. B-Layer) with staves, plus services for disks and staves. Total mass of system is 24.64kg; resultant frequency is 55.48Hz, in a lateral sway mode. As before, the rings do not contribute stiffness to the frame, as evidenced by their lack of their distortion.

Figure 13 shows data on four facilities, LIGO, Los Alamos National Laboratory Neutral Particle Beam and Laser Fusion Experiments, and a Neutral Particle Beam Experiment at

Argonne National Laboratory. Staff members at HYTEC were involved in taking the vibration data for the last three. The pre-LIGO construction data from an independent source was used by HYTEC in an early design phase for the LIGO seismic isolation system. LIGO without question is the quietest experimental hall that we have encountered. Recent LIGO data, now that the facility is near full operation, is reported to be somewhat higher, but still low in comparison to the other data. We use $10^{-6} \text{ G}^2/\text{Hz}$ over a frequency range of 10 to 500Hz. This range was taken to cover adequately the first 20 modes of frame vibration. The frame vibration eigenvalues range from 55.48 out to 200Hz.

A random vibration response solution will disclose to what extent each frame vibration mode will participate in the response. The solution method is a linear superposition of the individual normal modes with due regard to their modal participation. Out of the first 20 modes, involving X, Y, and Z motion, we fully expect some not to contribute much response. The response is determined by exciting the boundary nodes of the frame model with the input spectrum.

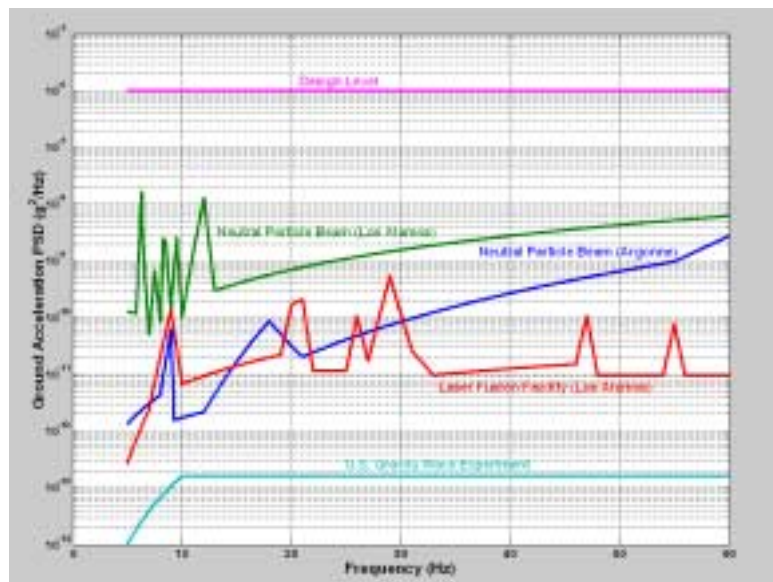


Figure 13: Comparison of design random vibration input PSD to levels recorded on specific experimental facilities. Design limit exceeds the highest recorded value by two orders of magnitude. Input to FEA is standard PSD format, acceleration squared per Hz.

Figure 14 depicts the PSD response for the constant input spectrum cited earlier. We see that the 1st mode, lateral sway, dominates. The higher frequency modes contribute in a small way to the overall response. Modifying the structure to raise or eliminate this mode is not expected to seriously increase the response of the higher modes above that shown.

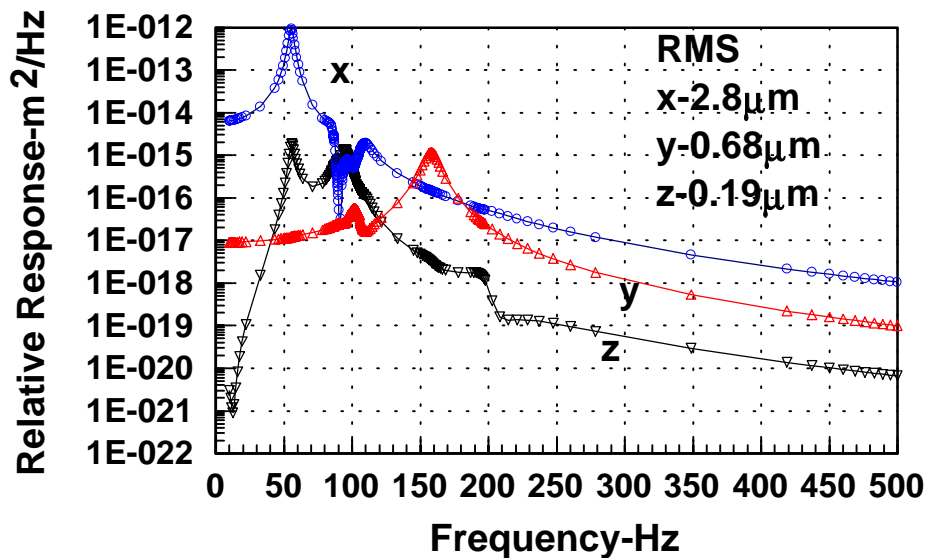


Figure 14: PSD Response (m^2/Hz) of Global Support Frame to random vibration input. Rms response of a node on end cone is $2.82\mu m$. RMS response at this point in the other directions, Y and Z, is less than $1\mu m$.

To complete the initial vibration study we need to consider the effect of encountering discrete vibration input spikes in the form of harmonic excitation. It is not uncommon for test equipment in an experimental hall to resonant when subjected to frequencies near their natural modes of vibration. It is conceivable that discrete harmonics will exist at the SCT/Pixel supports that will couple with the Pixel Detector structure. Frequencies of concern are 30, 60, and 120Hz. Again, we select a conservative input spectrum for excitation, based on the assumption that energy is not filtered by the SCT, but rather amplified. If we assume the input to be bounded by 0.001 to .01 G's the actual displacement excitation into the Pixel Detector will be of the order of 0.1 to $1\mu m$ at 50Hz. This level is conservative (hopefully).

Figure 16 depicts the response of the frame to the harmonic excitation. As anticipated, we see that most of the response is due to the 1st mode. The response at higher frequencies also is beneficially influenced by the decay in the input magnitude ($1/f^2$). A response peak of $11.8\mu m$ as shown in Figure 16 is certainly worrisome. We can draw little comfort from the fact the input is conservative. We must face the reality that with the present support boundary conditions that the frame fundamental frequency is too low, and that the ratio of the non-structural mass to structural mass is too high. We must face further the prospect that the magnitude of non-structural in Pixel Detector mass will increase. We observed before that this drop follows roughly the inverse square root of the percentage gain. If the detector mass reaches 34kg, the frequency will drop to nominally 46Hz. A review of the SCT documents will reveal that this value is very close to the 2nd SCT mode (54.4Hz), another undesirable condition.

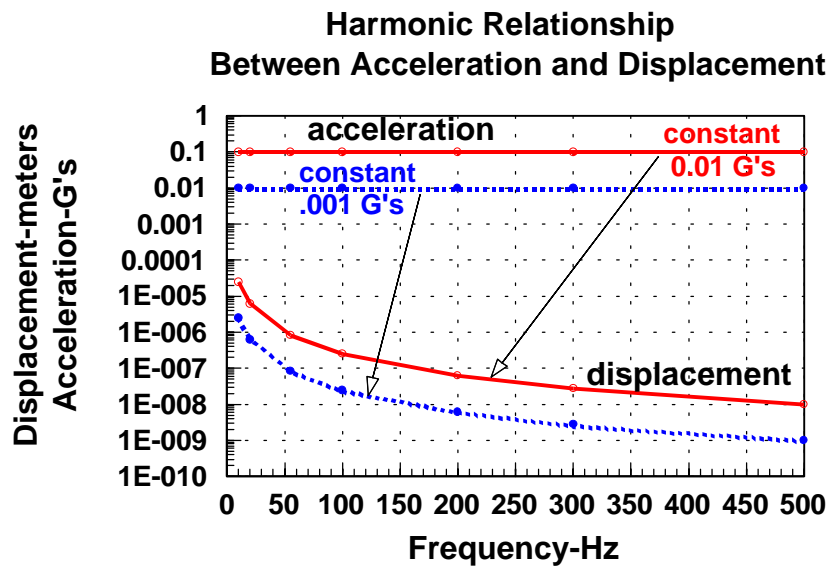


Figure 15: Input harmonic vibration curve for the Pixel Detector Global Support frame.

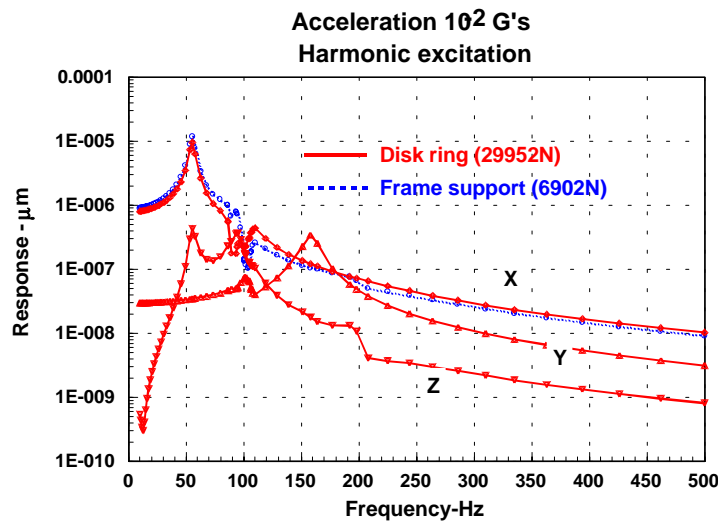


Figure 16: Global Support Structure harmonic response in X, Y, and Z from the harmonic excitation of Figure 15. Response at the frame fundamental mode is on the order of $10\mu\text{m}$

2.5 Global Support Assembly Static Solution

An assessment was made of the frame sag for the weight used in the vibration analysis, i.e., 24.64kg. The peak sag is $12\mu\text{m}$, slightly greater than for the larger 500mm dia support frame. Little can be done to decrease this value short of adding structural mass. This value is borderline acceptable, and it is sensitive to any further increase of non-structural mass.

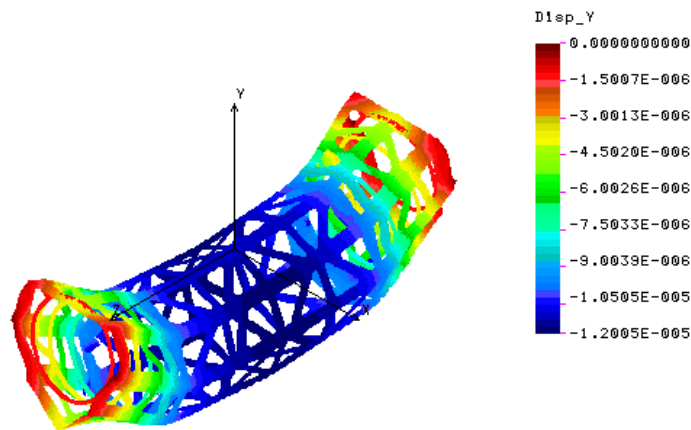


Figure 17: Gravity sag solution for Global Support Assembly, total mass of 24.64kg. Boundary conditions are same as represented in Figure 12, XYZ, XY, YZ, and Y. The peak sag is 12 μ m.

Figure 18 provides a measure of the torsional stiffness of the frame. Removing one support point allows racking and twisting of the frame, corresponding to essentially $\frac{1}{4}$ of the mass 6.16kgs (60.4N). This implies a torsional stiffness of 1.02 μ m/N or a corresponding angular stiffness of 5.55 μ rad/N. In summary, it is advisable to locate the 4-support points in a common plane to better than 25 μ m to avoid twisting the frame after assembly.

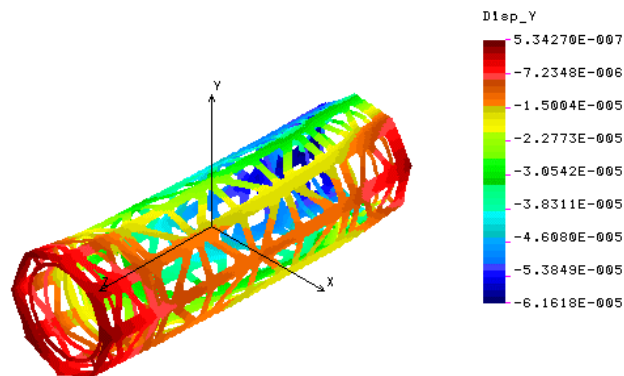


Figure 18: Global Support response to removing the single support Y. Three remaining supports fix the frame in XYZ, XY, and YZ. The upper right corner sags a maximum of 61.6 μ m.

2.6 Global Support Frame with an End Reinforcement Plate

2.6.1 Static Analysis of the End Plate Contribution

An argument was made that the frame natural frequency is low, potentially impacting the detector stability. The non-structural mass used in the FE model may also be low further, further stressing the need to raise the fundamental frame mode. To this end, an end plate reinforcement plate was added to the FE model. The plate is composed of an annular, sandwich plate with the same properties as used for the end cone flat, sandwich panels. The inner and outer radius of the

plate annulus is 101 and 160mm respectively. Eight, 4mm thick laminates, short extensions connect the annulus to the 8-outer frame corners. These short fingers would be constructed in the same fashion as used in the end cone to outer frame mounting tabs.

The purpose of the end plate is to contribute radial stiffness, thus their presence will do little for overcoming gravity sag. This fact is clearly shown in Figure 19 and Figure 20, where we note that the addition of the end plate in the model produced a very small reduction for the two gravity-sag loading conditions. The prior sag values were 12 and 61.6 μ m.

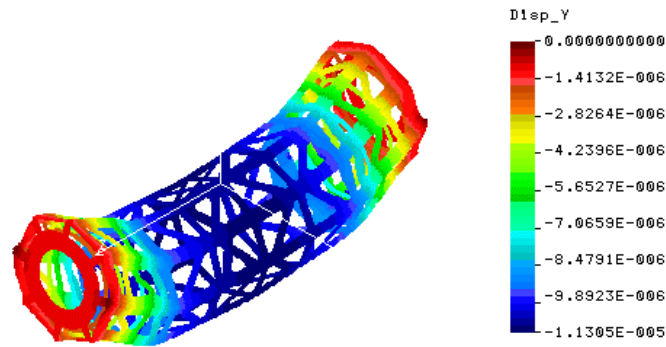


Figure 19: FEA solution of Global support Frame with reinforcing end plates used to raise the fundamental vibration mode. Gravitational sag for 1G loading in Y is 11.3 μ m. Boundary conditions are the standard 4-point corner support condition.

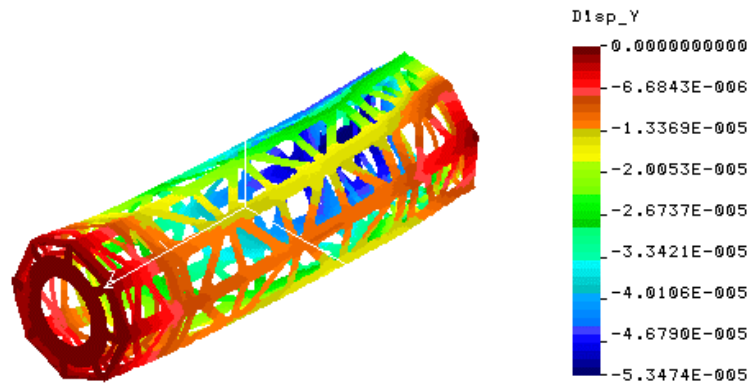


Figure 20: FEA solution with one of the 4-corner vertical support removed. Gravity sag causes a peak droop in the upper corner of 53.5 μ m.

2.6.2 Modal Analysis of the End Plate Contribution

A substantial increase in frame natural frequency is provided by the addition of the end plates. The lateral sway mode at 55.48Hz has been suppressed. The mode is a combination of an outer shell distortion and out-of-plane bending of the end cone. The major response of this mode is confined to the inner mounting surfaces of the end cone. All modes from 89 to 100Hz are

confined to the response of the end cone, and some of these may be suppressed if we added the inner barrel structures to our frame model.

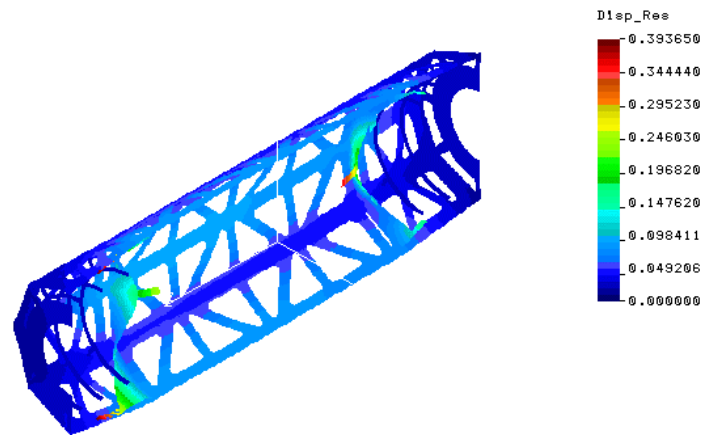


Figure 21: Cut-away showing the deformed shape for the fundamental mode of the modified Global Support Frame; two end reinforcement plates were added bringing the total system mass to 24.89kg. the 1st mode is characterized by an outer frame shell mode and end cone-bending mode.

3. Recommendations

The FEA studies of the Global Support frame point to the need of either over constraining the frame 4-point mount or adoption of an end plate reinforcement. The end plate reinforcement was evaluated and the result was quite positive in raising the fundamental mode. We recommend that end reinforcement be added to the frame. The addition of end reinforcement plate does not alleviate the need to secure close control on the planarity of the four mounting points for the frame. Whatever amount the four points are out-of-planarity, the frame will twist to come into contact. If one wishes to reduce the twist to much less than 50 μ m, one must bring the four mounts into a common plane to better than say 10 μ m. This requirement implies that one should give careful thought to the Global Support/Support Tube interface.